Thermochimica Acta, 182 (1991) 243–252
Elsevier Science Publishers B.V., Amsterdam

Thermally induced configurational and conformational changes of diamine complexes of nickel(II) trifluoromethanesulphonate

Sukumar Roy and Nirmalendu Ray Chaudhuri[1]

Department of Inorganic Chemistry, Indian Association for the Cultivation of Science, Calcutta 700 032 (India)

(Received 8 October 1990)

Abstract

The violet, octahedral complexes $[Ni(pn)_3](CF_3SO_3)_2$ (pn = 1,2-propanediamine), *trans*-$[NiL_2(H_2O)_2][(CF_3SO_3)_3$ (L = pn and 2,2-dimethyl-1,3-propanediamine(dmpd)), *cis*-$[Ni(mpn)_2(H_2O)_2](CF_3SO_3)_2$ (mpn = 2-methyl-1,2-propanediamine) and the yellow, square-planar complex $[Ni(ippn)_2](CF_3SO_3)_2$ (ippn = N^1-isopropyl-2-methyl-1,2-propanediamine) have been synthesized and their thermal reactions have been studied in the solid state. Upon heating, $[Ni(pn)_3](CF_3SO_3)_2$ undergoes an irreversible endothermic phase transition due to conformational changes of the diamine chelate ring. The complex *trans*-$[Ni(pn)_2(H_2O)_2]$ $(CF_3SO_3)_2$ shows thermochromism (violet → yellow) due to an octahedral → square-planar transformation, whereas *cis*-$[Ni(mpn)_2(H_2O)_2](CF_3SO_3)_2$ first shows thermochromism, like the pn complex and then, upon further heating, undergoes phase transitions due to conformational changes of the diamine chelate rings. However, *trans*-$[Ni(dmpd)_2(H_2O)_2](CF_3SO_3)_2$ shows a two-step thermochromism, violet → blue → yellow, corresponding to a diaquooctahedral → diaminooctahedral → square-planar transition. $[Ni(ippn)_2](CF_3SO_3)_2$ does not show any phase transition upon heating. The variation in thermal reactivities of the complexes can be understood on the basis of the steric hindrance caused by the substituent groups in the diamine.

INTRODUCTION

Thermochromic reactions in the solid state of transition metal compounds, mainly those of Cu(II) [1] and Ni(II) [1,2], are of great interest to chemists. Various mechanisms explaining the phenomenon of thermochromism have been proposed by several workers [3–6]. It has been observed that the basicity of the ligand, and the steric effect and coordinating ability of the anions are very important for a nickel(II) diamine complex in the solid-state thermal transformation octahedral → square-planar [2]. In continuation to our recent studies [7,8] relating to thermochromic transitions in

---

[1] Author to whom correspondence should be addressed.

nickel(II) diamine complexes, here CF_3CO_3 forms the anionic part of the complexes. This study with CF_3SO_3 anion forms is apparently meaningful because the anion has a moderate coordinating ability [9] and its bulkiness favours the square-planar → octahedral transformation for a nickel(II) diamine complex [2]. Its non-explosive nature is also most suitable for thermal application, compared with other bulky anions, e.g. ClO_4^-, NO_3^-, etc. In addition, the syntheses and characterisations of some metal complexes containing trifluoromethanesulphonate have been reported [10], although their thermal studies are not well documented [11]. Accordingly, we report here the results of the thermal investigations of nickel(II) trifluoromethanesulphonate complexes with some *C*-substituted diamines, although the occurrence of thermally induced conformational [12–14] and configurational [2,15] changes have been demonstrated in the solid state for a number of nickel(II) diamine complexes.

EXPERIMENTAL

High purity 1,2-propanediamine (pn), 2-methyl-1,2-propanediamine (mpn) and N^1-isopropyl-2-methyl-1,2-propanediamine (ippn) were purchased from Aldrich, and 2,2-dimethyl-1,3-propanediamine (dmpd) was from Fluka; both were used as received. All other chemicals used were AR grade.

The instruments employed for recording IR (ambient and above ambient temperature), TG–DTA, DSC, X-ray powder diffraction, magnetic susceptibility measurements and elemental analyses are as described in an earlier report [14]. The electronic spectra (recorded in a mull) in the N-IR region were measured on a Hitachi U-3400 spectrophotometer. Electronic spectral data, and the magnetic and thermal data are given in Tables 1 and 2, respectively.

TABLE 1

Magnetic moment and electronic spectral data (selected bands) of the complexes

Complex	Electronic spectra (nm)	Magnetic moment (B.M.)
$[Ni(pn)_3](CF_3SO_3)_2$ (**1**)	536, 370	3.1
$[Ni(pn)_3](CF_3SO_3)_2$ (**1a**)	536, 370	3.1
trans-$[Ni(pn)_2(H_2O)_2](CF_3SO_3)_2$ (**1b**)	1201, 783, 551	3.2
$[Ni(pn)_2](CF_3SO_3)_2$ (**1c**)	[a]	Diamagnetic
cis-$[Ni(mpn)_2(H_2O)_2](CF_3SO_3)_2$ (**2**)	919, 560	3.2
$[Ni(mpn)_2](CF_3SO_3)_2$ (**2a**)	[a]	Diamagnetic
$[Ni(mpn)_2](CF_3SO_3)_2$ (**2b**)	[a]	Diamagnetic
trans-$[Ni(dmpd)_2(H_2O)_2](CF_3SO_3)_2$ (**3**)	1197, 780, 560	3.1
$[Ni(dmpd)_2(CF_3SO_3)_2]$ (**3a**)	[a]	3.0
$[Ni(dmpd)_2](CF_3SO_3)_2$ (**3b**)	[a]	Diamagnetic
$[Ni(ippn)_2](CF_3SO_3)_2$ (**4**)	442	Diamagnetic

[a] It was not possible to record the electronic spectra of these complexes.

TABLE 2

Thermal parameters for the complexes

Thermal reactions	Temp. range (°C)	DSC peak temp (°C)		ΔH (kJ mol^{-1})
		Endo	Exo	
$[Ni(pn)_3](CF_3SO_3)_2$ (**1**) → $[Ni(pn)_3](CF_3SO_3)_2$ (**1a**)	202 –218	213.5	–	10.1
trans-$[Ni(pn)_2(H_2O)_2](CF_3SO_3)_2$ (**1b**) → $[Ni(pn)_2](CF_3SO_3)_2$ (**1c**)	57.5–122.5	107	–	77.7
$[Ni(pn)_2](CF_3SO_3)_2$ (**1c**) → $[Ni(pn)_2](CF_3SO_3)_2$ (**1c**)	–	240 [a]		–
cis-$[Ni(mpn)_2(H_2O)_2](CF_3SO_3)_2$ (**2**) → $[Ni(mpn)_2](CF_3SO_3)_2$ (**2a**)	52 –117	77(sh), 89	–	89.7
$[Ni(mpn)_2](CF_3SO_3)_2$ (**2a**) → $[Ni(mpn)_2](CF_3SO_3)_2$ (**2b**)	162.0–178.5	173	–	3.3
$[Ni(mpn)_2](CF_3SO_3)_2$ (**2b**) → $[Ni(mpn)_2](CF_3SO_3)_2$ (**2c**)	187 –204	193.5(sh), 198.5	–	7.9
$[Ni(mpn)_2](CF_3SO_3)_2$ (**2c**) → $[Ni(mpn)_2](CF_3SO_3)_2$ (**2b**)	191 –165	–	188, 172.5	–7.9
trans-$[Ni(dmpd)_2(H_2O)_2](CF_3SO_3)_2$ (**3**) → $[Ni(dmpd)_2(CF_3SO_3)_2]$ (**3a**)	62 –155	130	–	100.3
$[Ni(dmpd)_2(CF_3SO_3)_2]$ (**3a**) → $[Ni(dmpd)_2](CF_3SO_3)_2$ (**3b**)	160 –181	171	–	11.0
$[Ni(ippn)_2](CF_3SO_3)_2$ (**4**) → $[Ni(ippn)_2](CF_3SO_3)_2$ (**4**)	–	270 [a]		

[a] Peak due to melting; sh, shoulder.

Preparation of the complexes

The complexes [Ni(pn)$_3$](CF$_3$SO$_3$)$_2$ (**1**), *trans*-[Ni(pn)$_2$(H$_2$O)$_2$](CF$_3$SO$_3$)$_2$ (**1b**), *cis*-[Ni(mpn)$_2$(H$_2$O)$_2$](CF$_3$SO$_3$)$_2$ (**2**), *trans*-[Ni(dmpd)$_2$(H$_2$O)$_2$](CF$_3$SO$_3$)$_2$ (**3**) and [Ni(ippn)$_2$](CF$_3$SO$_3$)$_2$ (**4**), were prepared by mixing the respective diamine with nickel(II) trifluoromethanesulphonate in the correct ratio in ethanolic or aqueous medium. The desired complexes were formed by slow evaporation.

The complex [Ni(pn)$_3$](CF$_3$SO$_3$)$_2$ (**1a**) was synthesised by heating the parent complex (**1**) at 220 °C (Table 2). The complexes, [Ni(pn)$_2$](CF$_3$SO$_3$)$_2$ (**1c**), [Ni(mpn)$_2$](CF$_3$SO$_3$)$_2$ (**2a**), [Ni(mpn)$_2$](CF$_3$SO$_3$)$_2$ (**2b**), [Ni(dmpd)$_2$(CF$_3$SO$_3$)$_2$] (**3a**) and [Ni(dmpd)$_2$](CF$_3$SO$_3$)$_2$ (**3b**), were derived from their corresponding parent complexes at their respective formation temperatures (Table 2). Elemental analyses of the complexes are in good conformity with their compositions.

RESULTS AND DISCUSSION

Characterisation of the complexes

On the basis of the elemental analyses, the complexes have the following compositions: Ni(CF$_3$SO$_3$)$_2\cdot$(pn)$_3$ (**1**), Ni(CF$_3$SO$_3$)$_2\cdot$(pn)$_2\cdot$(H$_2$O)$_2$ (**1b**), Ni(CF$_3$SO$_3$)$_2\cdot$(mpn)$_2\cdot$(H$_2$O)$_2$ (**2**), Ni(CF$_3$SO$_3$)$_2\cdot$(dmpd)$_2\cdot$(H$_2$O)$_2$ (**3**) and Ni(CF$_3$SO$_3$)$_2\cdot$(ippn)$_2$ (**4**). The magnetic moment and electronic spectral data (Table 1) confirm the octahedral geometry of complexes (**1**), (**1b**), (**2**) and (**3**), and the square-planar geometry of (**4**). Furthermore, the mode of splitting of the d–d bands (Fig. 1 and Table 1) in the N-IR region indicates the *trans*-configurations of (**1b**) and (**3**) and the *cis*-configuration of (**2**) [15–17] and the complexes can be characterised as [Ni(pn)$_3$](CF$_3$SO$_3$)$_2$ (**1**), *trans*-[Ni(pn)$_2$(H$_2$O)$_2$](CF$_3$SO$_3$)$_2$ (**1b**), *cis*-[Ni(mpn)$_2$(H$_2$O)$_2$](CF$_3$SO$_3$)$_2$ (**2**), *trans*-[Ni(dmpd)$_2$(H$_2$O)$_2$](CF$_3$SO$_3$)$_2$ (**3**) and [Ni(ippn)$_2$](CF$_3$SO$_3$)$_2$ (**4**), respectively.

Phase transition in [Ni(pn)$_3$](CF$_3$SO$_3$)$_2$ (1)

Upon heating, complex (**1**) undergoes an irreversible endothermic phase transition without any visual colour change yielding its isomer (**1a**) (temp. range = 202–218 °C, $\Delta H = 10.1$ kJ mol^{-1}), see Table 2 and Fig. 2. The post-phase species (**1a**) retains its octahedral geometry as is evident from its magnetic and electronic spectral data (Table 2). However, the differences in the X-ray powder diffraction patterns and in the IR spectra in the regions 3340–2860, 1610–1000 and 470–340 cm^{-1} of the two isomers suggest probable conformational changes of the diamine chelate ring [12–14]. It has previously been observed that anions, e.g. BF$_4$, NO$_3$ [1,13], CF$_3$CO$_2$ [14],

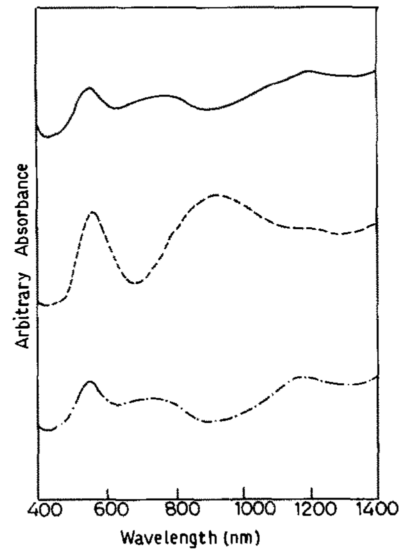

Fig. 1. Representative electronic spectra (*N*-IR–VIS region) of *trans*-$[Ni(pn)_2(H_2O)_2](CF_3SO_3)_2$ (**1b**) (———), *cis*-$[Ni(mpn)_2(H_2O)_2](CF_3SO_3)_2$ (**2**) (- - - - - -) and *trans*-$[Ni(dmpd)_2(H_2O)_2](CF_3SO_3)_2$ (**3**) (–·–·–).

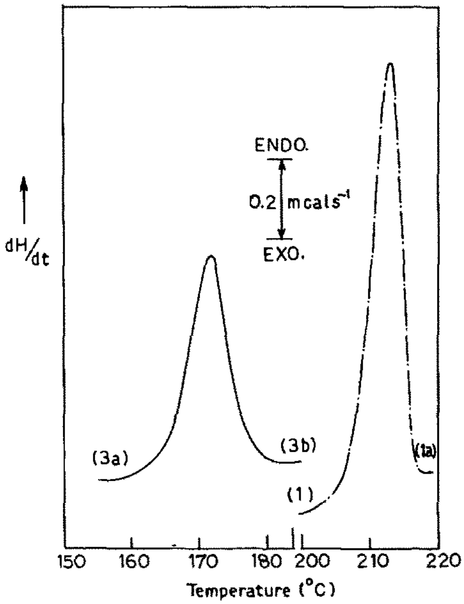

Fig. 2. DSC heating curves for the transformations of $[Ni(pn)_3](CF_3SO_3)_2$ (**1**) → $[Ni(pn)_3](CF_3SO_3)_2$ (**1a**) (sample mass, 8.6 mg) (–·–·–) and $[Ni(dmpd)_2(CF_3SO_3)_2]$ (**3a**) → $[Ni(dmpd)_2](CF_3SO_3)_2$ (**3b**) (sample mass, 5.6 mg) (———).

etc., are sometimes capable of forming hydrogen bonds with an amine hydrogen. Upon heating, the vibrations of both anion and diamine chelate ring would increase to reach a point where thermal energy weakens the H-bonding network, allowing the chelate ring to undergo a conformational change. Here, the anion CF_3SO_3 is expected to form a similar type of hydrogen bond. The considerably higher transition temperature and enthalpy value (in comparison to the analogous system $[Ni(diamine)_3]X_2$ where $X = BF_4$ or NO_3) [13] may be assumed to be due to the stronger hydrogen bonding. The post-phase species (**1a**), following prolonged standing either in open air or in a desiccator, does not revert to its pre-phase form, although the isomer (**1**) produces (**1a**) endothermically where the isomer (**1a**) is less stable energetically than (**1**). However, on crystallisation, (**1a**) reverts to (**1**).

Thermochromism in trans-*$[Ni(pn)_2(H_2O)_2](CF_3SO_3)_2$ (1b)*

Upon heating, the violet complex (**1b**) loses its water molecules yielding a yellow product, $[Ni(pn)_2](CF_3SO_3)_2$ (**1c**) (temp. range 57.5–122.5 °C, $\Delta H = 77.7$ kJ mol^{-1}) (Table 2). The yellow complex (**1c**) immediately transforms to (**1b**) in the open atmosphere but can be preserved in a desiccator. The magnetic moment of (**1c**) implies diamagnetism. It is apparent that the colour change from violet → blue is due to the octahedral → square-planar transformation. Upon further heating, the species (**1c**) melts (melting peak temp. 240 °C) (Table 2); on cooling in nitrogen, this solidifies to (**1c**) but yields the violet (**1b**) when cooled in an open atmosphere.

Thermochromic and non-thermochromic reactions in cis-*$[Ni(mpn)_2(H_2O)_2]$-$(CF_3SO_3)_2$ (2)*

Upon heating, the violet complex (**2**) becomes anhydrous at 117 °C yielding a yellow species, $[Ni(mpn)_2](CF_3SO_3)_2$ (**2a**) (temp. range 52–117 °C; $\Delta H = 89.7$ kJ mol^{-1}) (Table 2). The yellow anhydrous complex (**2a**), on cooling in open air, immediately transforms to (**2**). The magnetic moment of (**2a**) corroborates its square-planar geometry. Thus, here also, the colour change is due to the octahedral → square-planar transformation. It is interesting that the yellow, square-planar complex (**2a**), upon further heating, undergoes two endothermic transitions not associated with any colour change (temp. range 162–178.5 °C, $\Delta H = 3.3$ kJ mol^{-1} and temp. range 187–204 °C, $\Delta H = 7.9$ kJ mol^{-1}) which, on cooling, gives two exothermic peaks in the DSC curves (temp. range 191–165 °C (peak temp. = 188, 172.5 °C, respectively), $\Delta H = -7.9$ kJ mol^{-1}) (Table 2 and Fig. 3). DSC investigations in cyclic mode (temp. range = 160–205 °C) of the yellow complex (**2a**) show that the first endothermic peak at 173 °C is absent from the second and following heating curves, whereas the later transition (temp. range 187–204 °C) is observed unchanged in the second and third heating

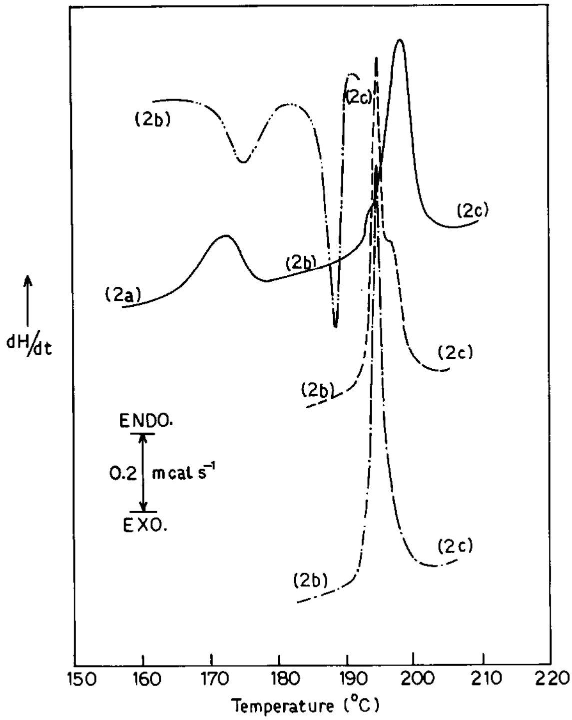

Fig. 3. DSC heating curves for the transformations of $[Ni(mpn)_2](CF_3SO_3)_2$ (**2a**) → $[Ni(mpn)_2](CF_3SO_3)_2$ (**2b**) → $[Ni(mpn)_2](CF_3SO_3)_2$ (**2c**) (1st heating (———), (**2b**) → (**2c**) (2nd heating) (- - - - - -), (**2b**) → (**2c**) (3rd heating/onward heating) (— · — · —), and (**2c**) → (**2b**) (1st/2nd/3rd/outward cooling) (— · · — · · —) (sample mass (same for all cases), 4.23 mg).

curves, although the third heating curve is found to be similar to subsequent heating curves. However, all the corresponding cooling curves are found to be identical, see Fig. 3, Table 2 and Scheme 1. The magnetic moment of the yellow species (isolated after the first transition, endothermic peak at 173 ° C) (Table 2) implies diamagnetism and, as with all the other transitions, none is associated with any colour change. Thus, it is apparent from the present and earlier studies [2,15] that all the yellow species should also be square-planar. We have recorded a large number of IR spectral runs for the former yellow species (isolated after the first endothermic transition) at 160 and 205 ° C, respectively, upon successive heating and cooling (temp. range 160–205 ° C) of the same sample; they show that the runs taken at each temperature are identical. This indicates that all the species present at each respective temperature are identical. The species present at 160 ° C is considered to be one variety (**2b**) with the other variety (**2c**) existing at 205 ° C. The IR spectrum of the species (**2a**) has also been recorded and, there are noticeable differences in the IR spectra of (**2a**), (**2b**) and (**2c**) in the regions 3350–3260 and 1280–940 cm^{-1}, which correspond to $\nu(NH_2)$, $\nu(CH_2)$ $(\tau(NH_2) + \rho_w(NH_2) + \tau(CH_2))$, $(\nu(C–N) + \nu(C–C))$ and $\rho_r(CH_2)$ vibrations, respec-

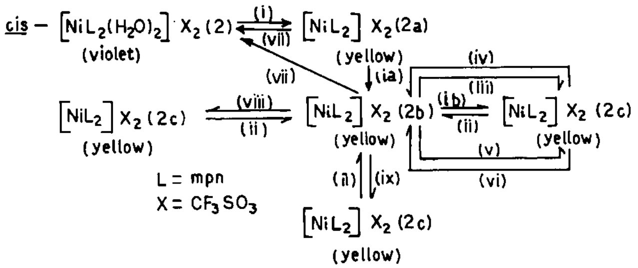

Scheme 1. (i) 1st heating (temp. range, 52–117 °C); (ia) 1st heating (temp. range, 162–178.5 °C, $\Delta H = 3.3$ kJ mol^{-1}); (ib) 1st heating, endotherms at 193.5° (sh) and 198.5 °C (peak) (temp. range, 187–204 °C, $\Delta H = 7.9$ kJ mol^{-1}); (ii) 1st cooling, exotherms at 188 and 172.5 °C (temp. range, 191–165 °C, $\Delta H = -7.9$ kJ mol^{-1}); (iii) 2nd heating, endotherms at 194.5 (peak) and 196.5 °C (sh) (temp. range, 185–202 °C, $\Delta H = 7.9$ kJ mol^{-1}); (iv) 2nd cooling, same as (ii); (v) 3rd, 4th and 5th heating, endotherms at 194.5 °C and a broad shoulder (temp. range, 185–202 °C, $\Delta H = 7.9$ kJ mol^{-1}); (vi) 3rd, 4th and 5th cooling, same as (ii); (vii) in humid atmosphere (relative humidity, 60–70%); (viii) sample (**2b**), isolated after (ia), kept at 160 °C for ≈ 2 h under N_2 atmosphere, DSC run same as (v); (ix) sample (**2b**), isolated after (v), kept at ≈ 50 °C for ≈ 6 h under N_2 atmosphere, DSC run follows (ib) → (iii) → (v) heatings with same cooling (ii).

tively [12–14]. These indicate that the species (**2a**), (**2b**) and (**2c**) are probably conformational isomers [12–14]. In this context it may be mentioned that the enthalpy changes for (**2b**) $\rightleftharpoons$ (**2c**) from all the heating/cooling curves are almost the same, although they were calculated manually from the respective peak areas. It is interesting that the species (**2b**) (derived directly from (**2**)) may be kept in the DSC sample-holder assembly in a nitrogen atmosphere at 160 °C for approximately 2 h. The thermal profiles for the phase transition (**2b**) → (**2c**) are always similar and appears identical to the third heating curve (Scheme 1). But when the species (**2b**) (isolated after the 3rd or subsequent heatings) is kept at approximately 50 °C for around 6 h, the same transition pattern shows similar variations as was observed in cyclic mode, as shown in Fig. 3. It is also interesting that the first endothermic transition at 173 °C is not reproducible, even following prolonged storage of the species (**2b**) in a dry atmosphere: this is only possible when (**2b**) is transformed to the aquated species (**2**).

Thermochromism in trans-*[Ni(dmpd)$_2$(H$_2$O)$_2$](CF$_3$SO$_3$)$_2$ (3)*

The violet complex (**3**) shows two-step thermochromism: violet → blue in the first step, and then blue → orange. The colour change in the first step corresponds to deaquation (temp. range 62–155 °C, $\Delta H = 100.3$ kJ mol^{-1}) (Table 2) and the second step is due to an endothermic transition without any mass loss in the corresponding TG curve (temp. range = 160–181 °C, $\Delta H = 11$ kJ mol^{-1}) (Table 2 and Fig. 1). The blue anhydrous species (**3a**) or the orange species (**3b**) immediately transforms to (**3**) following exposure in an open atmosphere. The magnetic moments of these species corroborate the octahedral geometry of (**3a**) and the square-planar geometry of (**3b**). Considering the composition and the geometry, (**3a**) and (**3b**) can be characterised as $[Ni(dmpd)_2(CF_3SO_3)_2]$ and $[Ni(dmpd)_2](CF_3SO_3)_2$, respectively. The mode of attachment of the CF_3SO_3 group in (**3a**) and (**3b**) could not be distinguished in the IR spectra due to the overlapping of diamine and CF_3SO_3 bands [9], although it is apparent that $CF_3SO_3^-$ is coordinated in (**3a**), whereas in (**3b**) it is not. So here the colour changes are due to a diaquooctahedral → diaminooctahedral → square-planar transformation. It is interesting that the orange product does not revert to the blue species upon cooling in nitrogen and remains unaffected by prolonged storage in nitrogen or in a desiccator.

The yellow, square-planar complex, $[Ni(ippn)_2](CF_3SO_3)_2$ (**4**) does not show any change upon heating but melts at 270 °C (melting peak temp.), like (**1c**) (Table 2).

We have tried to prepare the corresponding hydrated complex of (**4**) by changing the reaction medium and other experimental conditions but have failed to isolate any species other than its square-planar form. The tendency of ippn to favour the square-planar structure may be explained as follows. The presence of bulky substituents in ippn generates a large steric hindrance which possibly prevents the approach of other ligands in the axial direction. Moreover, due to the presence of alkyl substituents, the base strength of ippn is reasonably high which stabilises the square-planar structure [2].

Furthermore, it is seen that only the dmpd complex undergoes thermal anation. This can be explained by the magnitude of the inter-ligand steric repulsion which is expected to be relatively low in the dmpd (in comparison to the other diamines) because the two methyl substituents present in the C_2 position in dmpd are somewhat removed from the donor nitrogen atom.

The relative stability between (**3a**) and (**3b**) is interesting. Both species yield their corresponding hydrated analogue (**3**) when exposed to a humid atmosphere (Scheme 2), but the rate of transformation from (**3a**) to (**3**) is much faster than from (**3b**) to (**3**) in the same atmosphere (relative humidity = 60–70%). As mentioned above, when kept in nitrogen species (**3b**) never reverts to (**3a**), even after prolonged storage; it is also stable in a desiccator.

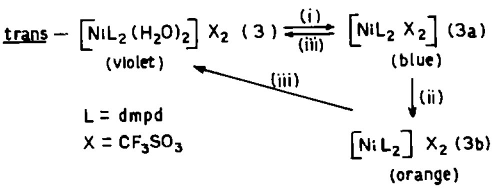

Scheme 2. (i) Temp. range, 62–155 °C; (ii) temp. range, 160–181 °C, $\Delta H = 11.0$ kJ mol^{-1}; (iii) in humid atmosphere (relative humidity, 60–70%).

From the above observations, it is apparent that (**3b**) is preferred over (**3a**). Here, the more populated complex (**3a**) is expected to be more sterically hindered than (**3b**) and from this point of view, this confirms the relatively higher stability of (**3b**) compared with (**3a**). But the corresponding thermal deanation reaction, i.e. (**3a**) → (**3b**), is endothermic, where the species (**3a**) is energetically more stable than (**3b**) by 11 kJ mol^{-1}, in contradiction to the above observations.

REFERENCES

1 D.R. Bloomquist and R.D. Willett, Coord. Chem. Rev., 47 (1982) 125.
2 E. Jona, J. Therm. Anal., 34 (1988) 1053.
3 A.B.P. Lever, E. Mantovani and J.C. Donini, Inorg. Chem., 10 (1971) 2424; A.B.P. Lever and E. Mantovani, Inorg. Chem., 10 (1971) 817.
4 I. Grenthe, P. Paoletti, H. Sandstorm and S. Glixberg, Inorg. Chem., 18 (1979) 2687.
5 M.M. Andino, J.D. Curet and M.M. Muir, Acta Crystallogr., 32B (1976) 3185.
6 W.E. Hatfield, T.S. Piper and V. Klabunde, Inorg. Chem., 2 (1963) 629.
7 S. Roy, A. Ghosh and N. Ray Chaudhuri, Transition Met. Chem., 14 (1989) 443.
8 S. Koner, A. Ghosh and N. Ray Chaudhuri, J. Chem. Soc., Dalton Trans., (1990) 1563.
9 A.R. Byington and W.E. Bull, Inorg. Chim. Acta, 21 (1977) 239.
10 G.A. Lawrance, Chem. Rev., 86 (1986) 17.
11 S.P. Mallela, R.A. Geanangel and W.W. Wendlandt, Thermochim. Acta, 156 (1989) 239.
12 G. De, P.K. Biswas and N. Ray Chaudhuri, J. Chem. Soc., Dalton Trans., (1984) 2591; A.K. Mukherjee, M. Mukherjee, A.J. Welch, A. Ghosh, G. De and N. Ray Chaudhuri, J. Chem. Soc., Dalton Trans., (1987) 997; S. Roy, G. De and N. Ray Chaudhuri, Bull. Chem. Soc. Jpn., 60 (1987) 2701.
13 S. Roy, A. Ghosh and N. Ray Chaudhuri, Thermochim. Acta, 136 (1988) 191; S. Roy, A. Ghosh and N. Ray Chaudhuri, Thermochim. Acta, 155 (1989) 297.
14 S. Roy, A. Ghosh and N. Ray Chaudhuri, Transition Met. Chem., 12 (1987) 453.
15 Y. Ihara, Y. Fukuda and K. Sone, Inorg. Chem., 26 (1987) 3745.
16 A.B.P. Lever, Inorganic Electronic Spectroscopy, 2nd. edn., Elsevier, Amsterdam, 1984, pp. 507–520.
17 Y. Ihara, Y. Fukuda and K. Sone, Bull. Chem. Soc. Jpn., 59 (1986) 1825.